European Journal of Physics

PAPER • OPEN ACCESS

A numerical damped oscillator approach to constrained Schrödinger equations

To cite this article: M Ögren and M Gulliksson 2020 *Eur. J. Phys.* **41** 065406

OPEN ACCESS
IOP Publishing
European Journal of Physics
Eur. J. Phys. **41** (2020) 065406 (18pp)
https://doi.org/10.1088/1361-6404/aba70b

A numerical damped oscillator approach to constrained Schrödinger equations

M Ögren[1,2,*] **and M Gulliksson**[1,3]

[1] School of Science and Technology, Örebro University, 701 82 Örebro, Sweden
[2] Hellenic Mediterranean University, PO Box 1939, GR-71004, Heraklion, Greece
[3] Institutt for data og realfag, Høgskulen på Vestlandet, 5020 Bergen, Norway

E-mail: magnus.ogren@oru.se and marten.gulliksson@oru.se

Received 18 March 2020, revised 6 July 2020
Accepted for publication 17 July 2020
Published 15 October 2020

Abstract

This article explains and illustrates the use of a set of coupled dynamical equations, second order in a fictitious time, which converges to solutions of stationary Schrödinger equations with additional constraints. In fact, the method is general and can solve constrained minimization problems in many fields. We present the method for introductory applications in quantum mechanics including three qualitative different numerical examples: the radial Schrödinger equation for the hydrogen atom; the 2D harmonic oscillator with degenerate excited states; and a nonlinear Schrödinger equation for rotating states. The presented method is intuitive, with analogies in classical mechanics for damped oscillators, and easy to implement, either with coding or with software for dynamical systems. Hence, we find it suitable to introduce it in a continuation course in quantum mechanics or generally in applied mathematics courses which contain computational parts. The undergraduate student can, for example, use our derived results and the code (supplemental material (https://stacks.iop.org/EJP/41/065406/mmedia)) to study the Schrödinger equation in 1D for any potential. The graduate student and the general physicist can work from our three examples to derive their own results for other models including other global constraints.

Keywords: Schrödinger equation, eigenenergies, degeneracy, nonlinear Schrödinger equation, constraints

S Supplementary material for this article is available online

(Some figures may appear in colour only in the online journal)

*Author to whom any correspondence should be addressed.

1. Introduction

In this article we describe the idea of solving stationary Schrödinger equations (SEs) as energy minimization problems with constraints, by using a second-order damped dynamical system. We discuss how to numerically solve the problems in a stable and efficient way.

For the formulas in this article to be easily recognized and directly applicable for the students in different courses, we write most formulas explicitly in an infinite-dimensional setting. For example, we use integrals instead of scalar products (or Dirac notation). However, if you write your own code[1] instead of using high-level solvers for the differential equations, you need to formulate integrals as finite sums and derivatives, e.g. as finite differences, i.e. the linear SE equation can be formulated as a linear eigenvector equation $Hu = Eu$, with H a matrix, u a (column) eigenvector, and E an eigenvalue of H.

We provide enough details, including the references, for all the numerical results presented here to be reproducible. We recommend that anyone who wants to use the method in practice, or who just wants to obtain a step-by-step understanding of the algorithm, should read (and run) the carefully implemented and commented codes provided [1].

From a pedagogical point of view, the method has the advantage of being able to solve a large set of problems in arbitrary dimensions with the same main idea.

The novel way we formulate constraints here allows for using high-level software instead of your own code, for example when calculating excited states.

There are of course many other ways of attaining the stationary solution of the SE numerically. For the common, so-called imaginary time dependent SE (see below), the approach is, after discretization in space (finite differences, finite elements, or other methods), to solve a first-order damped time dependent equation numerically, see [1, 2]. Sometimes these methods are called steepest descent methods (not to be confused with steepest descent methods in optimization [3]). In this category we also have the so-called shooting methods [4], although these are restricted to systems in one spatial dimension or with potentials obeying separation of variables. These are, in general, computationally expensive, but have some advantages for problems with complicated boundary conditions, and for problems with discontinuous solutions.

When the SE is independent of time (e.g. through separation of variables) the SE is, after discretization in space, equivalent to a (nonlinear) finite dimensional minimization problem, with nonlinear constraints. Generally, such minimization problems can be solved by a variety of numerical methods including gradient descent methods, (quasi-)Newton methods, machine learning techniques, etc [3, 5]. Note that in the linear case with only normalization constraints we have solved a linear eigenvalue problem, e.g. by so-called diagonalization [6], for which there are numerous specialized numerical methods.

Our method presented here can be used in a very general and efficient way for minimization problems (linear, nonlinear, with any type of global constraints) and has been shown to be highly competitive [7–9]. It can also be used for linear eigenvalue problems [10, 11].

We hope the readers will expand the theory and applications in different directions from the examples presented here.

[1] As a starting point for own coding, see supplementary material at https://stacks.iop.org/EJP/41/065406/mmedia, including: a simplified MATLAB program DFPM_1D_HO.m that can calculate excited states of a particle in a 1D harmonic oscillator potential; and DFPM_1D_NLSE.m that solves the NLSE as described in this article. Those codes can alternatively be used with the free software OCTAVE, https://gnu.org/software/octave/.

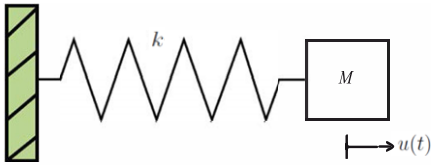

Figure 1. A simple oscillating spring–mass system.

2. The method

In order to introduce the idea of the method let us first consider a basic example in classical mechanics. The harmonic oscillator is, according to Newton's second law, described by

$$M\ddot{u} + ku = 0, \quad k > 0. \tag{1}$$

Here $u = u(t)$ is the distance from the equilibrium for a mass M on which a force $F = -ku$ is acting. The dot denotes the time derivative. For example, the mass could be attached to a spring, with k being the spring constant, see figure 1. If we in addition assume that there is some linear resistance proportional to the velocity $\dot{u}$, e.g. between the mass and the surface on which it is sliding, we get a damped second-order system

$$M\ddot{u} + \eta\dot{u} - F(u) = 0, \tag{2}$$

where $\eta > 0$ is a damping parameter due to the linear resistance. With the damping term present the kinetic energy will decay with time, such that $M\ddot{u} + \eta\dot{u} \to 0$ when $t \to \infty$. It is clear from this example that one of the parameters M, η, k can be scaled out, so we usually set $M = 1$ in the following. The solutions of equation (2) in the noncritical case ($\eta \neq 2\sqrt{k}$) are given by

$$u(t) = C_1 \ \exp(\xi_1 t) + C_2 \ \exp(\xi_2 t), \tag{3}$$

where C_i are determined by the initial conditions $u(0)$ and $\dot{u}(0)$, and $\xi_j = -\eta/2 \pm \sqrt{(\eta/2)^2 - k}$. It is easy to see from equation (3) that u tends to zero when t goes to infinity, which is the equilibrium position of the mass and hence the stationary solution to equation (2). The value $\eta = 2\sqrt{k}$ for the damping parameter ensures the ξ_j is real and is referred to as critical damping for equation (2), for which $u(t) = (C_1 + C_2 t) \ \exp(-\sqrt{k}t)$. For smaller or larger values of η, the oscillations are referred to as under- or over-damped, respectively. The critically damped system is known to be the fastest way for the system to return to its equilibrium, i.e., to reach the stationary solution. In multimode discretized systems the above argument can be generalized in order to obtain an optimal value for the damping parameter to be used in a numerical calculation [7].

Now we note that $u = 0$ is also the solution of the (trivial) minimization problem $\min\left(ku^2/2\right)$. In fact, the convex functional $V(u) = ku^2/2$ is the mechanical potential corresponding to the force $F = -ku$ which is conservative, i.e., $F = -\mathrm{d}V/\mathrm{d}u$. Of course, in this case it is easier to directly solve $ku = 0$ or $\min ku^2/2$ for u, than to integrate the differential equation (2). However, this simple idea can be extended to solve more challenging problems, where η takes the role of a parameter that can be tuned for optimal numerical properties, as we explain in this article.

2.1. Damped oscillator approach to the ground state of the Schrödinger equation

We here briefly repeat how the stationary (i.e. time-independent) SE for a particle with mass M and a spatially-dependent potential $V(\mathbf{r},t) = V(\mathbf{r})$ is attained from the time-dependent SE:

$$\mathrm{i}\hbar\frac{\partial\Psi}{\partial t} = -\frac{\hbar^2}{2M}\nabla^2\Psi + V\Psi \equiv \hat{H}\Psi. \tag{4}$$

Given a time- and space-separating ansatz of the wavefunction $\Psi(\mathbf{r},t) = u(\mathbf{r})\exp(-\mathrm{i}Et/\hbar)$, we then have from equation (4):

$$\hat{H}u = Eu. \tag{5}$$

Alternatively, the stationary SE can be viewed as the Euler–Lagrange equation [12] corresponding to the minimization of the energy, which, if we start from equation (5), is the following functional of u:

$$E(u) = \frac{\int \bar{u}\hat{H}u\mathrm{d}\mathbf{r}}{\int |u|^2\mathrm{d}\mathbf{r}}, \tag{6}$$

where the bar from now on denotes complex conjugation.

If the normalization of the wave function is considered as a constraint, then the denominator of equation (6) is unity and the ground state of equation (5) is given by the solution of

$$E = \min_u \int \bar{u}\hat{H}u\mathrm{d}\mathbf{r}, \quad \text{s.t.} \int |u|^2\mathrm{d}\mathbf{r} = 1, \tag{7}$$

where s.t. is an abbreviation for 'subject to'. We later give examples with more complicated constraints.

Our main idea for solving equation (7) is to mimic equation (2) and consider the second-order damped dynamical system:

$$\ddot{u} + \eta\dot{u} + \frac{\delta E}{\delta\bar{u}} = 0, \quad \eta > 0, \qquad \int |u|^2\mathrm{d}\mathbf{r} = 1. \tag{8}$$

In the following we reserve the dot notation for the derivatives with respect to a fictitious time τ. The force F in equation (2) corresponds to the generalized force $-\delta E/\delta\bar{u}$, the third term in equation (8), i.e., to a functional derivative of the energy. It can be shown [13] that the stationary solution to equation (8), say $u^*(\mathbf{r})$, is the solution to equation (7). Note that in the limit when $\tau \to \infty$ the stationary solution u^* will satisfy the Euler–Lagrange equation $\delta E/\delta\bar{u} = 0$. The corresponding energy is $E(u^*) = \min_u\left(\int \bar{u}\hat{H}u\mathrm{d}\mathbf{r}\right)$ where $\hat{H}$ is the Hamiltonian operator from the SE (4).

After the problem has been formulated as in equation (8), an important question is the following: how do we choose a stable and efficient numerical method for obtaining the stationary solution to equation (8)? Symplectic integration methods [14] are tailor-made for Hamiltonian systems. This serves as the motivation for our choice of numerical method. Let us rewrite equation (8) as the first-order system

$$\begin{aligned} \dot{u} &= v \\ \dot{v} &= -\eta v - \frac{\delta E}{\delta\bar{u}}. \end{aligned} \tag{9}$$

Then, we can apply a symplectic explicit method, such as symplectic Euler or Störmer–Verlet [14], which gives us an iterative map in the numerical approximations $(u_\nu, v_\nu), \nu = 1, 2, 3, \ldots$

with a step in fictitious time $\Delta\tau_\nu$ and damping η_ν. The choice of parameters $\Delta\tau_\nu$ and η_ν can be chosen in order to optimize the performance of the numerical method, which is generally a nontrivial task. However, for linear differential equations, such as the SE, analytical results exist [7, 10]. For simplicity, we will keep all parameters constant through the iterations, i.e. independent of the step ν.

The approach of finding the solution to equation (7) by solving equation (8) with a symplectic method has been named the dynamical functional particle method (DFPM) [11]. We would like to emphasize that it is the combination of the second-order damped dynamical system together with an efficient (fast, stable, accurate) symplectic solver that makes the DFPM a very powerful method. Even if the idea of solving minimization problems using dynamical systems with different damping strategies goes far back, see references [15, 16], it has not been presented for the SE with constraints with symplectic solvers for second-order systems. According to our practical experience many common (non-symplectic) integration methods with optimal or nonoptimal damping parameters give a reasonably fast convergence of equation (8) to the stationary solutions. So, unless the numerical performance is important, a variety of softwares for dynamical systems can be used in practical implementations.

Let us finally comment on one closely related approach for solving equation (7) that has been studied extensively [1, 2], namely, *the steepest descent method*:

$$\dot{u} + \alpha\frac{\delta E}{\delta \bar{u}} = 0, \quad \alpha > 0, \qquad \int |u|^2 \mathrm{d}\mathbf{r} = 1. \tag{10}$$

The method is called the imaginary time method when applied to the SE with $\alpha = 1$ (i.e. change $t \to -\mathrm{i}\tau$ in equation (4)). It might seem that equation (10) is better than equation (8) since the exponential decrease towards the stationary solution in equation (10) can be made arbitrarily large by choosing α large enough. However, as proven strictly for linear problems [7], and by numerical evidence for some nonlinear examples [9], going to a second-order differential equation in a fictitious time is superior if one takes into account the stability and accuracy of the numerical solver. DFPM has been shown to have a remarkably faster convergence to the stationary solution than any numerical method applied to equation (10), see [7].

It is the purpose of this article to explain this new method through a few qualitatively different examples for the stationary SE. In addition, it will be extended to a corresponding method to treat constraints.

2.2. Damped oscillator approach for global constraints

DFPM is readily extended to more general constrained problems, e.g. normalized and excited states of the SE in general settings. Consider a convex minimization problem for $E(u)$ with smooth global constraint functionals $G_j(u) = 0$, i.e.

$$\min_u E(u), \quad \text{s.t. } G_j(u) = 0. \tag{11}$$

The actual choice of index j is dependent on what is natural for different problem settings. To give one example of a constraint, $G_j(u) = 0$, the normalization constraint in equation (7) can be written in this form, see equation (14).

The problem in equation (11) has a unique solution u^* if $\delta G_j/\delta\bar{u}$ is surjective at u^*, and thus fulfils the so-called Karush–Kuhn–Tucker conditions. The corresponding dynamical system for constraints can be formulated using an extended constrained energy functional (often called Lagrange function in mathematical literature) $I(u, \mu_1, \mu_2, \ldots) = E(u) + \sum_j \mu_j G_j(u)$, where μ_j

are Lagrange multipliers. The dynamical system for solving equation (11) is then given by

$$\ddot{u} + \eta\dot{u} + \frac{\delta E}{\delta \bar{u}} + \sum_j \mu_j \frac{\delta G_j}{\delta \bar{u}} = 0, \tag{12}$$

with $\mu_j(\tau)$ chosen such that $u(\tau)$ tends to the stationary solution u^* when τ tends to infinity, see examples in the next section. For more details on the existence and uniqueness of solutions to constrained problems see [17] and references therein.

In order to solve equation (11) one can choose the $\mu_j(\tau)$ such that $u(\tau)$ always remains on the constraints set, e.g. by projection methods, or as we will do here, to approach the constraints set (usually in an oscillatory manner) as τ increases. Projection is generally costly but there are important exceptions such as, e.g. eigenvalue problems with only normalization constraints.

For our damped approach, we introduce an additional dynamical system, analogous to equations (2) and (8), for a constraint G_j as in equation (11) according to

$$\ddot{G}_j + \eta\dot{G}_j + k_j G_j = 0, \quad \eta > 0,\ k_j > 0. \tag{13}$$

Note that equation (13) describes damped oscillators. Then $G_j(u(\tau))$ tends to zero exponentially fast and equation (13) can be used to derive expressions of the Lagrange multipliers $\mu_j(\tau)$ for equation (12), which for some problems are explicit, see further details in sections 3.1 and 3.2.

This method, based on equation (13), was introduced in [10] for solving matrix eigenvalue problems, where it was shown that $u(\tau)$ converges asymptotically to the eigenvectors. It was also shown that the choice of k_j in equation (13) does not change the local convergence rate if k_j lie within a rather large range which is determined by the eigenvalues to the operator $\delta E/\delta \bar{u}$, see [10] for details. In this article we always keep $k_j = k$ for all j for simplicity, while using the freedom in different k_j can further improve the numerical performance of the method.

Under these assumptions, the local convergence rate of the corresponding symplectic Euler with the optimal parameters [7] will be the same as for the projection approach. However, while the two approaches have the same local behavior it is not generally known *a priori* which of these two methods is faster for a specific problem. Further, note that a general known disadvantage with projection is that large changes in the Lagrange multipliers require small timesteps.

3. Two examples of constraints with explicit derivations of Lagrange multiplicators

We include two examples of constraints here in detail for readers who wish to understand the method. We begin by deriving the Lagrange multiplier for only one normalization constraint, then we add only an orthogonalization constraint, i.e. what is needed to calculate the first excited state of the SE.

3.1. Normalization constraint

Taking the first- and second-order derivatives of the normalization constraint

$$G_1 = 1 - \int |u|^2 \mathrm{d}\mathbf{r} \equiv 1 - N(\tau) = 0, \tag{14}$$

with respect to τ gives

$$\dot{G}_1 = -\int \left(\dot{\bar{u}}u + \bar{u}\dot{u}\right) \mathrm{d}\mathbf{r}, \qquad \ddot{G}_1 = -\int \left(\ddot{\bar{u}}u + 2\dot{\bar{u}}\dot{u} + \bar{u}\ddot{u}\right) \mathrm{d}\mathbf{r}. \tag{15}$$

Inserting the expressions from equation (15) into the left hand side of the general differential equation for constraints (13), then gives, after simplifications,

$$\ddot{G}_1 + \eta\dot{G}_1 = -\int \left(\left\{\ddot{\bar{u}} + \eta\dot{\bar{u}}\right\} u + \bar{u}\left\{\ddot{u} + \eta\dot{u}\right\} + 2|\dot{u}|^2\right) \mathrm{d}\mathbf{r}. \tag{16}$$

If we now use the DFPM equation (12) with $\delta E/\delta\bar{u} + \mu_1\delta G_1/\delta\bar{u} = \hat{H}u - \mu_1 u$ for the stationary SE. We can then, when $\ddot{u} + \eta\dot{u} \to 0$, identify the limit of the Lagrange multiplier being equal to the energy, $\lim_{\tau\to\infty} \mu_1(\tau) = E$, compare with equation (5). Inserting $-\hat{H}u + \mu_1 u$ into the curly brackets of equation (16) gives, after simplifications,

$$\ddot{G}_1 + \eta\dot{G}_1 = 2E - 2\mu_1 N - 2\int |\dot{u}|^2 \mathrm{d}\mathbf{r} = -k_1(1-N), \tag{17}$$

with $E(\tau) \equiv \int \bar{u}\hat{H}u \,\mathrm{d}\mathbf{r}$. Finally we can solve for the Lagrange multiplier $\mu_1(\tau)$

$$\mu_1 = \frac{E + k_1(1-N)/2 - \int |\dot{u}|^2 \mathrm{d}\mathbf{r}}{N}. \tag{18}$$

We see in equation (18) that $\mu_1 \to E$, since $|\dot{u}| \to 0$, $N \to 1$ as $\tau \to \infty$.

3.2. Normalization constraint and one orthogonalization constraint

Introducing, in addition to G_1 above, the following orthogonalization constraint:

$$G_0 = \int \bar{u}u_0 \mathrm{d}\mathbf{r} = 0, \tag{19}$$

means that the solution u, should be orthogonal to a known normalized function u_0. This u_0 can be defined analytically, which can be helpful while testing software[1], but more often u_0 is a numerically obtained approximation. For example, in the case of a convex 1D problem, u_0 is the solution with the lowest eigenvalue E (ground state), and u is the solution with the second lowest eigenvalue E (first excited state). As seen in the 2D example of section 4.2, this situation can be more complicated in higher dimensions where eigenvalues can be degenerate, meaning that several different solutions can have the same eigenvalue.

Taking the first- and second-order derivatives with respect to τ of the orthogonalization constraint in equation (19) gives

$$\dot{G}_0 = \int \dot{\bar{u}}u_0 \mathrm{d}\mathbf{r}, \qquad \ddot{G}_0 = \int \ddot{\bar{u}}u_0 \mathrm{d}\mathbf{r}. \tag{20}$$

Inserting the expressions from equations (19) and (20) into the general differential equation for constraints (13), then gives, with simplifications,

$$\ddot{G}_0 + \eta\dot{G}_0 = \int \left\{\ddot{\bar{u}} + \eta\dot{\bar{u}}\right\} u_0 \mathrm{d}\mathbf{r} = \int \left\{-\hat{H}\bar{u} + \mu_1\bar{u}\right\} u_0 \mathrm{d}\mathbf{r} - \mu_0 = -k_0 G_0. \tag{21}$$

In comparison to equation (17) there is now an additional term ($j = 0$) in equation (12). The corresponding coupled equation for G_1 is

$$\ddot{G}_1 + \eta\dot{G}_1 = 2E - 2\mu_1 N + \int \left(\mu_0\bar{u}_0 u + \mu_0\bar{u}u_0 - 2|\dot{u}|^2\right) \mathrm{d}\mathbf{r} = -k_1 G_1. \tag{22}$$

Finally, we write equations (21) and (22) for the two coupled Lagrange multipliers $\mu_0(\tau)$ and $\mu_1(\tau)$ as a linear system

$$\begin{bmatrix} 1 & -G_0 \\ -\mathrm{Re}\,(G_0) & 1 - G_1 \end{bmatrix} \begin{bmatrix} \mu_0 \\ \mu_1 \end{bmatrix} = \begin{bmatrix} k_0 G_0 - \int u_0 \hat{H}\bar{u}\mathrm{d}\mathbf{r} \\ E - \int |\dot{u}|^2 \mathrm{d}\mathbf{r} + k_1 G_1/2 \end{bmatrix} \equiv \begin{bmatrix} y_1 \\ y_2 \end{bmatrix}, \tag{23}$$

where $\mathrm{Re}\,(G_0) = \int (\bar{u}_0 u + \bar{u}u_0)\,\mathrm{d}\mathbf{r}/2$. We can check the limits for the Lagrange multipliers from equation (23), i.e. $\mu_0 \to 0$ and $\mu_1 \to E$, since $\dot{u} \to 0$, $G_0 \to 0$, $G_1 \to 0$ as $\tau \to \infty$.

Using Cramer's rule on the linear system of equation (23) gives the explicit expressions

$$\mu_0 = \frac{(1 - G_1)y_1 + G_0 y_2}{1 - G_1 - G_0 \mathrm{Re}\,(G_0)}, \qquad \mu_1 = \frac{y_2 + \mathrm{Re}\,(G_0)\, y_1}{1 - G_1 - G_0 \mathrm{Re}\,(G_0)}, \tag{24}$$

that can be used to calculate the first excited state in various problems.

In appendix A, we show how an arbitrary number of orthogonalization constraints are treated. We stress that the obtained result from appendix A can be used for SEs in any dimension with any potential, as illustrated in sections 4.1 and 4.2.

4. Numerical examples

In this section we show numerical results using the symplectic Euler method [14] for three examples and compare the presented DFPM method against analytic formulas. The first example is a linear equation in one radial variable for the hydrogen atom. The second is a harmonic oscillator in two variables (2D), which gives degenerated solutions. Finally, an example of a nonlinear Schrödinger equation (NLSE) is given.

4.1. The radial equation for the hydrogen atom

The function u is, in this example, the radial part of the 3D spatial wavefunction from equation (4), but multiplied with the radius $r = |\mathbf{r}|$, i.e. $\tilde{u}(\mathbf{r}) = \tilde{u}(r, \theta, \phi) = u(r)/r\, Y_l^m(\theta, \phi)$, where Y_l^m are the spherical harmonics. We write the dimensionless (i.e. with $\hbar = M_\mathrm{e} = a_0 = 1$) radial SE of the hydrogen atom as

$$\hat{H}_{(r)} u \equiv -\frac{1}{2}\frac{\mathrm{d}^2 u}{\mathrm{d}r^2} + \left(\frac{l\,(l+1)}{2r^2} - \frac{1}{r}\right) u = Eu, \qquad 4\pi \int_0^\infty |u|^2 \mathrm{d}r = 1, \tag{25}$$

where the expression within the large parenthesis in equation (25) is referred to as the effective radial potential. The factor 4π in the normalization constraint comes from the radial symmetry in 3D. For comparison, the energies only depend on a single quantum number $n = 1, 2, 3, \ldots$ and are given by [18]

$$E_n = -\frac{M_\mathrm{e} e^4}{2(4\pi\varepsilon_0)^2\hbar^2}\frac{1}{n^2} = -\frac{\hbar^2}{2M_\mathrm{e} a_0^2}\frac{1}{n^2} = -\frac{1}{2}\frac{1}{n^2}, \tag{26}$$

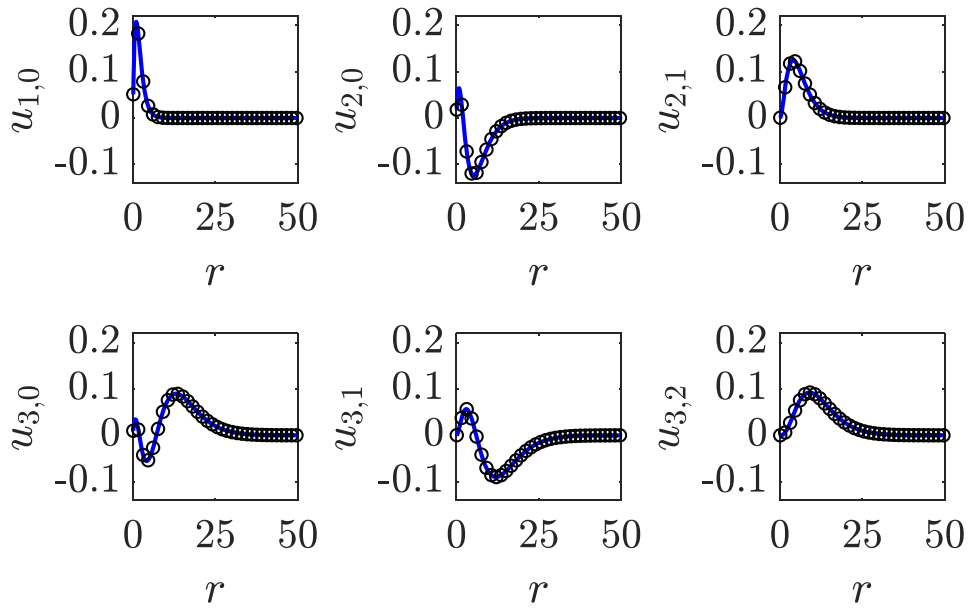

Figure 2. The six numerical solutions of equation (28) with the lowest energies E. Solid (blue) curves are numerical results, while (black) circles show the result of equation (27). We used an equidistant grid $10^{-6} < r_j < 10^2$, $j = 1, \ldots, 10^3$, and $\tau_{\max}$ large enough such that $|\ddot{u} + \eta\dot{u}| < 10^{-6}$ in equation (12). DFPM parameters used were $\eta = 0.5$, $k = 4$, and $\Delta\tau = 0.1$, which are of the same order of magnitude as the optimal predicted values for linear systems [7]. The (real) initial condition $u(0)$ was in this example chosen randomly. We note that the sign of the final wavefunction depends on the initial condition used.

where $a_0 = 4\pi\varepsilon_0\hbar^2/(M_e e^2)$ is a length scale called the Bohr radius. The corresponding radial wavefunctions depend on the two quantum numbers $n = 1, 2, 3, \ldots$ and $l = 0, 1, 2, \ldots, n-1$ and are given by [18]

$$u_{n,l}(r)/r = \sqrt{\frac{1}{\pi a_0^3 n^4}\frac{(n-l-1)!}{(n+l)!}}\left(\frac{2r}{na_0}\right)^l L_{n-l-1}^{2l+1}\left(\frac{2r}{na_0}\right)\exp\left(-\frac{r}{na_0}\right), \quad (27)$$

where L denotes the generalized Laguerre polynomials [19], defined in agreement with the MATLAB command `laguerreL(n - l - 1, 2*l + 1, 2*r/n)`, although different normalization factors can be found in the physics literature.

The effective radial potential in equation (25) depends on the quantum number l, as do the solutions in equation (27), so there is not any degeneracy when solving equation (25) numerically. In other words, the solution of equation (25) is unique for this radial SE. However, all states with the same quantum number n have the same energy E, as is clear from equation (26), and together with the degeneracy $(2m + 1)$ for the spherical harmonics Y_l^m, the three-dimensional wavefunction for hydrogen have a n^2 degeneracy.

The solutions u_{n,l^*} with $n = 1, 2, \ldots, n^* - 1$ should be orthogonal to the unknown u_{n^*,l^*}. Since u_{n,l^*}, $n = 1, 2, \ldots, n^* - 1$ are needed in order to obtain u_{n^*,l^*}, we solve equation (12) in consecutive order. More specifically, we start with the normalization constraint, see section 3.1, to obtain u_{1,l^*}, then add an orthogonality constraint, see section 3.2, to obtain u_{2,l^*}, and generally several orthogonality constraints, see appendix A, to obtain the solutions u_{n^*,l^*} with $n^* > 2$.

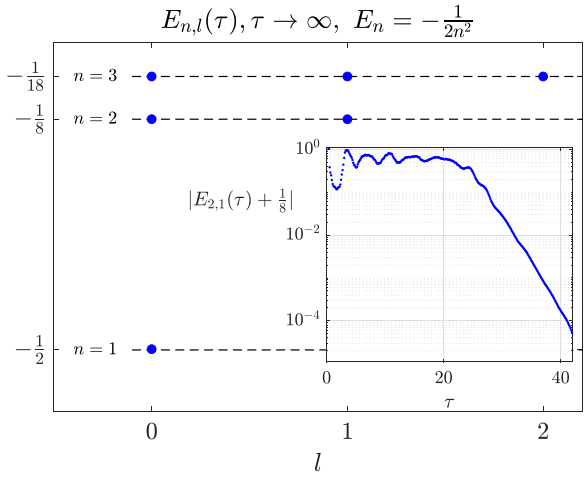

Figure 3. The six lowest energies E for the hydrogen atom. Dots (blue) are the numerically calculated energies from equation (28). The dashed horizontal (black) lines correspond to the values from equation (26). The inset figure shows the convergence dynamics of the energy $E_{2,1}$ as a function of the fictitious time. The parameters used are the same as the one in the caption of figure 2.

We can write the n^* constraints compactly using the Kronecker delta as $G_n = 4\pi \int_0^\infty \bar{u}_{n^*,l^*} u_{n,l^*} \mathrm{d}r - \delta_{n^*,n} = 0, \quad n = 1, 2, \ldots, n^*$. Using equation (25) we formulate the dynamical system, different for each value of l^*, that is, equation (12) applied to this radial SE is

$$\ddot{u}_{n^*,l^*} + \eta \dot{u}_{n^*,l^*} + \hat{H}_{(r)}(l^*) u_{n^*,l^*} + \sum_{n=1}^{n^*} \mu_n \frac{\delta G_n}{\delta \bar{u}} = 0. \tag{28}$$

The two Lagrange multipliers needed in the sum above to calculate the first excited state, i.e. for $n^* = 2$, can be obtained from equation (24). For the case with several multipliers ($n^* > 2$) in equation (28), they can conveniently be obtained from, e.g. numerical solutions of equation (A.6).

The six stationary numerical solutions to equation (28) with lowest energies are plotted in figure 2, while the corresponding energies are illustrated in figure 3.

4.2. Two-dimensional harmonic oscillator

In this example we calculate the well-known wave functions $u(x, y)$ and energies E to the dimensionless (i.e. with $\hbar = M = \omega = 1$) SE with an isotropic two-dimensional harmonic potential on a 2D Cartesian grid:

$$\hat{H}u \equiv -\frac{1}{2}\left(\frac{\partial^2}{\partial x^2} + \frac{\partial^2}{\partial y^2}\right) u + \frac{1}{2}\left(x^2 + y^2\right) u = Eu \int_{\mathbb{R}^2} |u|^2 \mathrm{d}\mathbf{r} = 1. \tag{29}$$

That is, for the ground state we solve the following optimization problem:

$$\min_u \int_{\mathbb{R}^2} \bar{u}\hat{H}u \mathrm{d}\mathbf{r}, \quad \text{s.t.} \int_{\mathbb{R}^2} |u|^2 \mathrm{d}\mathbf{r} = 1. \tag{30}$$

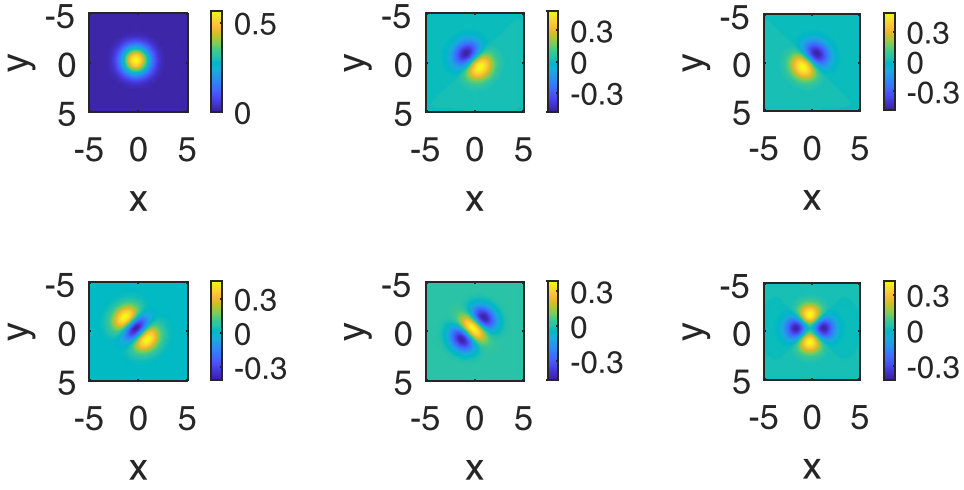

Figure 4. The six numerical wavefunctions of equation (32), with the lowest energies E. We used $-5 \leqslant x, y \leqslant 5$ and $\Delta x = \Delta y = 1/12$ for the discretization, which is enough to obtain all six solutions with correct energies within three significant digits. The parameters were $\eta = 1.5, k = 0.5$ and $\Delta\tau = 0.05$, which is in the same order of magnitude as predicted to be optimal [7]. The initial wavefunction (for all six subfigures here) was a translated and scaled (unnormalized) Gaussian $u(\tau = 0) = 1.2/\sqrt{\pi}\ \exp(-((x-1.2)^2 + (y-1.2)^2)/2)$ with $E(\tau = 0) \simeq 2.5$ (see the left ring in figure 5). The six numerical wavefunctions, from the upper left subfigure to the bottom right subfigure, correspond to $u_{(n_x,n_y)}$ from equation (33) in the order $(n_x, n_y) = (0,0), (1,0), (0,1); (2,0), (0,2), (1,1)$. However, note that the orientation and phase (sign) of the final wavefunction depends on the initial condition used.

Let u_s denote the sth eigenstate and $E_s = \int_{\mathbb{R}^2} \bar{u}_s \hat{H} u_s \mathrm{d}\mathbf{r}$ the corresponding eigenvalue. To obtain u_{s^*} for $s^* > 1$ we use, in addition to equation (29), the $s^* - 1$ orthogonality constraints

$$\int_{\mathbb{R}^2} \bar{u}_{s^*} u_1 \mathrm{d}\mathbf{r} = 0, \int_{\mathbb{R}^2} \bar{u}_{s^*} u_2 \mathrm{d}\mathbf{r} = 0, \ldots, \int_{\mathbb{R}^2} \bar{u}_{s^*} u_{s^*-1} \mathrm{d}\mathbf{r} = 0. \tag{31}$$

Using equations (29) and (31) we can from equation (12) formulate the corresponding dynamical system with the s^* constraints $G_s = \int_{\mathbb{R}^2} \bar{u}_{s^*} u_s \mathrm{d}\mathbf{r} - \delta_{s^*,s} = 0$, $s = 1, 2, \ldots, s^*$, as

$$\ddot{u}_{s^*} + \eta \dot{u}_{s^*} + \hat{H} u_{s^*} + \sum_{s=1}^{s^*} \mu_s \frac{\delta G_s}{\delta \bar{u}} = 0. \tag{32}$$

Since one needs access to $u_s, s = 1, 2, \ldots, s^* - 1$, we solve equation (32) in consecutive order. The two Lagrange multipliers needed in the sum above to calculate the first excited state, i.e. for $s^* = 2$, are given by equation (24). For the case with several multipliers ($s^* > 2$) in equation (32), see appendix A, they can conveniently be obtained from, for example, numerical solutions of equation (A.6). We show the six first numerical solutions to equation (32) in figure 4.

For comparisons, we note that equation (29) has the explicit solutions [18]

$$u_{(n_x,n_y)}(x,y) = \frac{1}{\sqrt{2^{(n_x+n_y)} n_x! n_y! \pi}} \mathcal{H}_{n_x}(x)\, \mathcal{H}_{n_y}(y) \exp\left(-\frac{x^2+y^2}{2}\right), \tag{33}$$

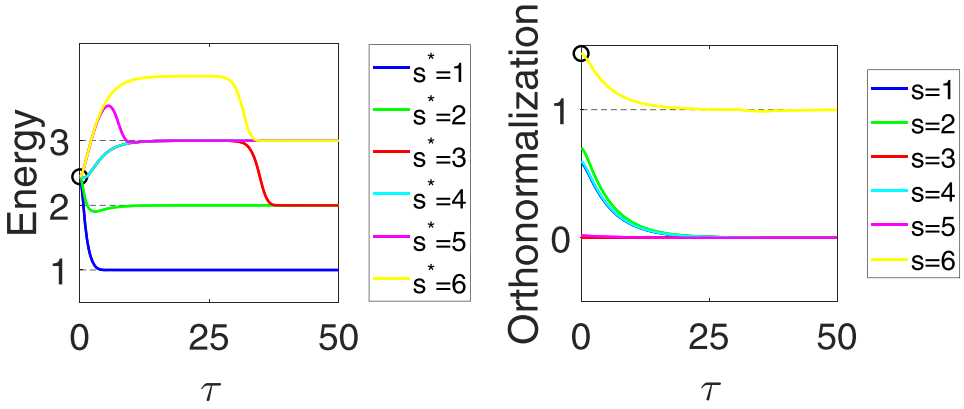

Figure 5. Left figure: Convergence of the energies for the six solutions seen in figure 4. Dashed horizontal lines correspond to the exact energies $E_{(n_x,n_y)} = n_x + n_y + 1$. Right figure: Illustration of the convergence of the calculation for solution number six (i.e. $s^* = 6$ corresponding to $n_x = n_y = 1$). The uppermost curve shows the normalization $\int |u|^2 \mathrm{d}\mathbf{r}$ (the ring shows the value $1.2^2 = 1.44$, see the initial condition in the caption of figure 4), and the lower curves show the five orthogonality constraints $\int \bar{u} u_s \mathrm{d}\mathbf{r}$, $s = 1, 2, 3, 4, 5$.

where $\mathcal{H}$ denote the Hermite polynomials [19], and the two quantum numbers can take the values $n_x, n_y = 0, 1, 2, 3, \ldots$.

In contrast to the radial SE for the hydrogen atom, there is no dependence on any of the quantum numbers n_x, n_y in the SE (29), and different solutions $u_{(n_x,n_y)}$ can give degenerate energies $E_{(n_x,n_y)} = n_x + n_y + 1$ as long as $n_x + n_y$ is constant.

In the left plot of figure 5 we show the numerical convergence for the energies. In the right plot of figure 5 we show the numerical convergence for the constraints.

4.3. The NLSE under rotation

The NLSE is commonly used to model many interacting bosonic particles via a mean-field approximation [20]. We have developed a DFPM formulation with damped constraints for a dimensionless NLSE in $u = u(x)$ on a ring geometry $-\pi \leqslant x \leqslant \pi$ ($R = \hbar = 2M = 1$) using periodic boundary conditions $u(-\pi) = u(\pi)$.

The aim is to minimize the total energy

$$E(u) = \int_{-\pi}^{\pi} \left| \frac{\partial u}{\partial x} \right|^2 + \pi\gamma |u|^4 \, \mathrm{d}x, \tag{34}$$

with γ a parameter for the nonlinear term, subject to one constraint for normalization, and one constraint for the angular momentum being ℓ_0

$$G_1 = 1 - \int_{-\pi}^{\pi} |u|^2 \mathrm{d}x = 0, \qquad G_2 = \ell_0 + \mathrm{i} \int_{-\pi}^{\pi} \bar{u} \frac{\partial u}{\partial x} \, \mathrm{d}x = 0. \tag{35}$$

We note that this problem can be solved analytically and refer to appendix B of reference [9] for the details of the solutions. In earlier work we implemented DFPM numerically for this problem with a modified RATTLE method [9], in which we solved for the two Lagrange multipliers corresponding to equation (35) numerically in each timestep. There it was demonstrated

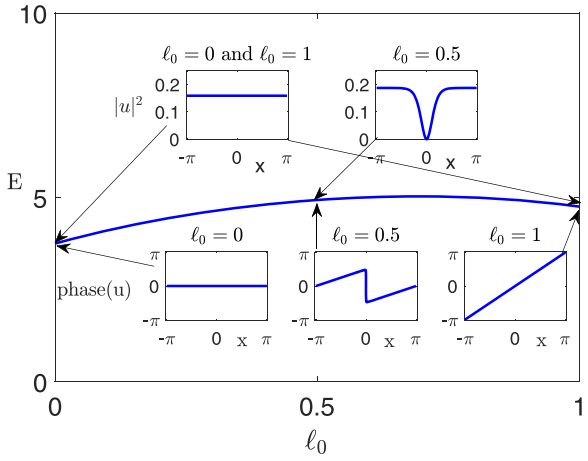

Figure 6. Yrast curve [9], i.e. energy vs momentum, with some examples of the density and the phase for the wavefunction u for the constant of nonlinearity being $\gamma = 7.5$. Optimal numerical parameters in equation (36) are not trivially given in the nonlinear case, and we used $\eta = k/2 = 1$ and $\Delta\tau = 0.015$. The spatial equidistant discretization consisted of 400 points.

that DFPM outperformed another commonly used method that is first order in time [9]. In this article we instead couple the minimization of equation (34) to equation (35), via the dynamical equation (13) for the constraints and get the following realization of equation (12):

$$\ddot{u} + \eta\dot{u} + \frac{\delta E}{\delta \bar{u}} + \mu\frac{\delta G_1}{\delta \bar{u}} + \Omega\frac{\delta G_2}{\delta \bar{u}} = \ddot{u} + \eta\dot{u} - \frac{\partial^2 u}{\partial x^2} + 2\pi\gamma|u|^2 u - \mu u + \mathrm{i}\Omega\frac{\partial u}{\partial x} = 0, \quad (36)$$

with the two Lagrange multipliers from equation (B.10):

$$\mu = \frac{b_1\langle\hat{\ell}^2\rangle - b_2\ell}{N\langle\hat{\ell}^2\rangle - \ell^2}, \qquad \Omega = \frac{b_2 N - b_1\ell}{N\langle\hat{\ell}^2\rangle - \ell^2}. \quad (37)$$

The Lagrange multipliers in equations (36) and (37) represent physical properties. Hence, μ is the so-called chemical potential, which is not equal to the energy E for the NLSE, and Ω is the angular velocity for the rotation. The quantities N, $\langle\hat{\ell}^2\rangle$, ℓ, b_1, b_2 in equation (37), which depend on the fictitious time τ, are defined in appendix B.

In figure 6 we have plotted the resulting so-called Yrast curve (main figure) with the density and phase of the corresponding complex wave function u for the particularly interesting points $\ell_0 = 0, 0.5, 1$ (inset figures). At integer values of ℓ_0 (0, 1 in this example), u is a plane-wave $u = \exp(\mathrm{i}\ell_0 x)/\sqrt{2\pi}$. At half-integer values (e.g. $\ell_0 = 0.5$), u corresponds to a dark solitary wave that circulates in the ring [21], see the right-upper- and mid-lower-inset figures.

5. Conclusions

We have introduced the DFPM with normalization and several orthogonalization constraints for the linear SE. Numerical results are presented for the wavefunctions and energies of the radial part of the hydrogen atom, and for the 2D harmonic oscillator. Furthermore, DFPM was formulated with constraints for rotational states to the NLSE and then solved numerically.

We believe this presentation of DFPM may be helpful for students and researchers who want to solve globally constrained equations in general. More specifically, it can be used for numerically solving different kinds of SE attaining (degenerated) excited states and energies.

Obviously, DFPM will not outperform all existing methods for solving the large variety of different SEs. However, as partly discussed in the introduction, we here mention four general advantages that we believe are of importance: (1) the method has a general formulation and can solve many different kinds of problems; (2) among methods for solving equations with ordinary differential equations DFPM seems to be the best; (3) we have here specifically shown that DFPM is relevant and competitive for several important problems in quantum mechanics; and (4) the method is simple to implement: discretize in space then solve the second-order damped dynamical system with a stable method, preferably a symplectic method; see the codes in the supplementary material.

Acknowledgements

We acknowledge valuable comments from Patrik Sandin, and from two anonymous referees. We also thank the three 'French musketeers' Julien Régnier, Nico Gaudy, and Alexandre Clercq for valuable discussions about DFPM during their internships at Örebro University.

Appendix A. Normalization constraint and several orthogonalization constraints

In the numerical examples in sections 4.1 and 4.2 both a normalization constraint and several orthogonalization constraints are treated simultaneously. We here sketch how an arbitrary number of orthogonalization constraints is treated. The result will hold for any potential $V(\mathbf{r})$ in any dimension.

We generalize equations (14) and (19) to a vector containing w orthogonalization constraints and one normalization constraint

$$\vec{G} = \begin{bmatrix} \int \bar{u}u_0 \mathrm{d}\mathbf{r} \\ \int \bar{u}u_1 \mathrm{d}\mathbf{r} \\ \vdots \\ \int \bar{u}u_{w-1} \mathrm{d}\mathbf{r} \\ 1 - \int \bar{u}u \mathrm{d}\mathbf{r} \end{bmatrix} = \vec{0}. \tag{A.1}$$

Hence with

$$\dot{\vec{G}} = \begin{bmatrix} \int \dot{\bar{u}}u_0 \mathrm{d}\mathbf{r} \\ \int \dot{\bar{u}}u_1 \mathrm{d}\mathbf{r} \\ \vdots \\ \int \dot{\bar{u}}u_{w-1} \mathrm{d}\mathbf{r} \\ -\int \dot{\bar{u}}u + \bar{u}\dot{u} \mathrm{d}\mathbf{r} \end{bmatrix}, \ddot{\vec{G}} = \begin{bmatrix} \int \ddot{\bar{u}}u_0 \mathrm{d}\mathbf{r} \\ \int \ddot{\bar{u}}u_1 \mathrm{d}\mathbf{r} \\ \vdots \\ \int \ddot{\bar{u}}u_{w-1} \mathrm{d}\mathbf{r} \\ -\int \ddot{\bar{u}}u + \bar{u}\ddot{u} + 2\dot{\bar{u}}\dot{u} \mathrm{d}\mathbf{r} \end{bmatrix}, \tag{A.2}$$

we have from equation (13)

$$\ddot{\vec{G}} + \eta\dot{\vec{G}} = \begin{bmatrix} \int \left(\ddot{\bar{u}} + \eta\dot{\bar{u}}\right) u_0 \mathrm{d}\mathbf{r} \\ \int \left(\ddot{\bar{u}} + \eta\dot{\bar{u}}\right) u_1 \mathrm{d}\mathbf{r} \\ \vdots \\ \int \left(\ddot{\bar{u}} + \eta\dot{\bar{u}}\right) u_{w-1} \mathrm{d}\mathbf{r} \\ -\int \left\{\ddot{\bar{u}} + \eta\dot{\bar{u}}\right\} u + \left\{\ddot{u} + \eta\dot{u}\right\} \bar{u} + 2\dot{\bar{u}}\dot{u}\mathrm{d}\mathbf{r} \end{bmatrix} = \begin{bmatrix} -k_0 G_0 \\ -k_1 G_1 \\ \vdots \\ -k_{w-1} G_{w-1} \\ -k_w G_w \end{bmatrix}. \quad \text{(A.3)}$$

From equation (12) we now have

$$\ddot{\bar{u}} + \eta\dot{\bar{u}} = -\hat{H}\bar{u} - \sum_{j=0}^{w-1} \mu_j \bar{u}_j + \mu_w \bar{u}, \quad \text{(A.4)}$$

with $\hat{H} = -\frac{\hbar^2}{2M}\nabla^2 + V(\mathbf{r})$ as defined in equation (4), such that the left-hand side of equation (A.3) is

$$\ddot{\vec{G}} + \eta\dot{\vec{G}} = \begin{bmatrix} -\int u_0 \hat{H}\bar{u}\mathrm{d}\mathbf{r} + \mu_w \int \bar{u}u_0 \mathrm{d}\mathbf{r} - \sum_{j=0}^{w-1} \mu_j \int \bar{u}_j u_0 \mathrm{d}\mathbf{r} \\ -\int u_1 \hat{H}\bar{u}\mathrm{d}\mathbf{r} + \mu_w \int \bar{u}u_1 \mathrm{d}\mathbf{r} - \sum_{j=0}^{w-1} \mu_j \int \bar{u}_j u_1 \mathrm{d}\mathbf{r} \\ \vdots \\ -\int u_{w-1} \hat{H}\bar{u}\mathrm{d}\mathbf{r} + \mu_w \int \bar{u}u_{w-1} \mathrm{d}\mathbf{r} - \sum_{j=0}^{w-1} \mu_j \int \bar{u}_j u_{w-1} \mathrm{d}\mathbf{r} \\ 2E + 2\mu_w (G_w - 1) + \sum_{j=0}^{w-1} \mu_j \int \left(\bar{u}_j u + \bar{u}u_j\right) \mathrm{d}\mathbf{r} - 2\int \dot{\bar{u}}\dot{u}\mathrm{d}\mathbf{r} \end{bmatrix}. \quad \text{(A.5)}$$

Now since $\int \bar{u}_i u_j \mathrm{d}\mathbf{r} = \delta_{ij}$ we can write equation (A.3) in matrix form with the Lagrange multipliers as the unknowns

$$\begin{bmatrix} 1 & 0 & \dots & 0 & -G_0 \\ 0 & 1 & \dots & 0 & -G_1 \\ \vdots & \vdots & & \vdots & \vdots \\ 0 & 0 & \dots & 1 & -G_{w-1} \\ -\mathrm{Re}\,(G_0) & -\mathrm{Re}\,(G_1) & \dots & -\mathrm{Re}\,(G_{w-1}) & 1 - G_w \end{bmatrix} \begin{bmatrix} \mu_0 \\ \mu_1 \\ \vdots \\ \mu_{w-1} \\ \mu_w \end{bmatrix}$$

$$= \begin{bmatrix} k_0 G_0 - \int u_0 \hat{H}\bar{u}\mathrm{d}\mathbf{r} \\ k_1 G_1 - \int u_1 \hat{H}\bar{u}\mathrm{d}\mathbf{r} \\ \vdots \\ k_{w-1} G_{w-1} - \int u_{w-1} \hat{H}\bar{u}\mathrm{d}\mathbf{r} \\ k_w G_w/2 + E - \int |\dot{u}|^2 \mathrm{d}\mathbf{r} \end{bmatrix}, \quad \text{(A.6)}$$

where $\mathrm{Re}\left(G_j\right) = \int \left(\bar{u}_j u + \bar{u} u_j\right) \mathrm{d}\mathbf{r}/2$ and $E = \int \bar{u}\hat{H}u \, \mathrm{d}\mathbf{r}$.

For example, with only one ($w = 1$) orthogonality constraint, equation (A.6) is the system in equation (23).

We note that the system (A.6) can be solved very efficiently by sparse Gaussian elimination with a computational cost proportional to w.

Appendix B. Normalization and angular momentum constraints

The two constraints we used for the NLSE are defined in equation (35). Taking the first- and second-order derivatives of G_1 and G_2 with respect to τ gives

$$\dot{G}_1 = -\int_{-\pi}^{\pi} \left(\dot{\bar{u}}u + \bar{u}\dot{u}\right) \mathrm{d}x, \qquad \ddot{G}_1 = -\int_{-\pi}^{\pi} \left(\ddot{\bar{u}}u + 2\dot{\bar{u}}\dot{u} + \bar{u}\ddot{u}\right) \mathrm{d}x, \tag{B.1}$$

respectively

$$\dot{G}_2 = \mathrm{i}\int_{-\pi}^{\pi} \left(\dot{\bar{u}}\frac{\partial u}{\partial x} + \bar{u}\frac{\partial \dot{u}}{\partial x}\right) \mathrm{d}x, \qquad \ddot{G}_2 = \mathrm{i}\int_{-\pi}^{\pi} \left(\ddot{\bar{u}}\frac{\partial u}{\partial x} + 2\dot{\bar{u}}\frac{\partial \dot{u}}{\partial x} + \bar{u}\frac{\partial \ddot{u}}{\partial x}\right) \mathrm{d}x. \tag{B.2}$$

Inserting the expressions from equations (B.1) and (B.2) into the left-hand side of the general differential equation for constraints (13), then gives after simplifications

$$\ddot{G}_1 + \eta\dot{G}_1 = -\int_{-\pi}^{\pi} \left(\left\{\ddot{\bar{u}} + \eta\dot{\bar{u}}\right\} u + \bar{u}\left\{\ddot{u} + \eta\dot{u}\right\} + 2|\dot{u}|^2\right) \mathrm{d}x, \tag{B.3}$$

and

$$\ddot{G}_2 + \eta\dot{G}_2 = \mathrm{i}\int_{-\pi}^{\pi} \left(\left\{\ddot{\bar{u}} + \eta\dot{\bar{u}}\right\}\frac{\partial u}{\partial x} + \bar{u}\left\{\frac{\partial \ddot{u}}{\partial x} + \eta\frac{\partial \dot{u}}{\partial x}\right\} + 2\dot{\bar{u}}\frac{\partial \dot{u}}{\partial x}\right) \mathrm{d}x. \tag{B.4}$$

The use of equation (36) for the curly brackets above gives (with η, γ, μ and Ω real, and by using integration by parts to some terms)

$$\ddot{G}_1 + \eta\dot{G}_1 = \int_{-\pi}^{\pi} \left(-2\bar{u}\frac{\partial^2 u}{\partial x^2} + 4\pi\gamma|u|^4 + 2\mathrm{i}\Omega\bar{u}\frac{\partial u}{\partial x} - 2\mu|u|^2 - 2|\dot{u}|^2\right) \mathrm{d}x, \tag{B.5}$$

and

$$\begin{aligned}\ddot{G}_2 + \eta\dot{G}_2 = \int_{-\pi}^{\pi} \Bigg(&2\mathrm{i}\frac{\partial u}{\partial x}\frac{\partial^2 \bar{u}}{\partial x^2} - 2\mathrm{i}\pi\gamma|u|^2\bar{u}\frac{\partial u}{\partial x} - 2\mathrm{i}\pi\gamma\bar{u}\frac{\partial\left(|u|^2 u\right)}{\partial x} + 2\Omega\bar{u}\frac{\partial^2 u}{\partial x^2} \\ &+ 2\mathrm{i}\mu\bar{u}\frac{\partial u}{\partial x} + 2\mathrm{i}\dot{\bar{u}}\frac{\partial \dot{u}}{\partial x}\Bigg) \mathrm{d}x.\end{aligned} \tag{B.6}$$

Comparing the above equations with equation (13) and inserting the constraints (35)

$$G_1 = 1 - \int_{-\pi}^{\pi} |u|^2 \mathrm{d}x \equiv 1 - N = 0, \qquad G_2 = \ell_0 + \mathrm{i}\int_{-\pi}^{\pi} \bar{u}\frac{\partial u}{\partial x} \, \mathrm{d}x \equiv \ell_0 - \ell = 0, \tag{B.7}$$

with the three real functions $N(\tau)$, $\ell(\tau)$ and $\langle\hat{\ell}^2\rangle(\tau) = -\int_{-\pi}^{\pi} \bar{u}\frac{\partial^2 u}{\partial x^2} \, \mathrm{d}x$, being the norm, the angular momentum, and (here) the kinetic energy, respectively, we have from equation (B.5)

$$-2N\mu - 2\ell\Omega + \int_{-\pi}^{\pi} \left(-2\bar{u}\frac{\partial^2 u}{\partial x^2} + 4\pi\gamma|u|^4 - 2|\dot{u}|^2\right) \mathrm{d}x = -k_1 G_1, \tag{B.8}$$

and from equation (B.6)

$$-2\ell\mu - 2\langle\hat{\ell}^2\rangle\Omega + \int_{-\pi}^{\pi}\left(2\mathrm{i}\frac{\partial u}{\partial x}\frac{\partial^2\bar{u}}{\partial x^2} - 4\mathrm{i}\pi\gamma\frac{\partial u}{\partial x}|u|^2\bar{u} - 2\mathrm{i}\pi\gamma\frac{\partial(\bar{u}u)}{\partial x}\bar{u}u + 2\mathrm{i}\dot{\bar{u}}\frac{\partial\dot{u}}{\partial x}\right)\mathrm{d}x = -k_2G_2. \tag{B.9}$$

The second to last term in the left-hand side above disappears, since $\int\frac{\partial(\bar{u}u)}{\partial x}\bar{u}u\mathrm{d}x = \int\frac{\partial}{\partial x}(\bar{u}u)^2\,\mathrm{d}x/2 = \left(|u(\pi)|^4 - |u(-\pi)|^4\right)/2 = 0$ due to the periodic boundary conditions. Hence, equations (B.8) and (B.9) lead us to the following linear system for the Lagrange multipliers:

$$\begin{bmatrix} N & \ell \\ \ell & \langle\hat{\ell}^2\rangle \end{bmatrix}\begin{bmatrix}\mu\\ \Omega\end{bmatrix} = \begin{bmatrix} k_1G_1/2 + \int_{-\pi}^{\pi}\bar{u}\hat{H}u\,\mathrm{d}x - \int_{-\pi}^{\pi}|\dot{u}|^2\,\mathrm{d}x \\ k_2G_2/2 - \mathrm{i}\int_{-\pi}^{\pi}\frac{\partial u}{\partial x}\hat{H}\bar{u}\,\mathrm{d}x + \mathrm{i}\int_{-\pi}^{\pi}\bar{\dot{u}}\frac{\partial\dot{u}}{\partial x}\,\mathrm{d}x \end{bmatrix} \equiv \begin{bmatrix} b_1\\ b_2\end{bmatrix}, \tag{B.10}$$

where $\hat{H}u = \delta E/\delta\bar{u}$ with E from equation (34). Using Cramer's rule on the above linear system gives the explicit expressions used in equation (37).

ORCID iDs

M Ögren https://orcid.org/0000-0002-2630-7479

References

[1] Schroeder D V 2017 The variational-relaxation algorithm for finding quantum bound states *Am. J. Phys.* **85** 698
[2] Smyrlis G and Zisis V 2004 Local convergence of the steepest descent method in Hilbert spaces *J. Math. Anal. Appl.* **300** 436
[3] Nocedal J and Wright S J 2006 *Numerical Optimization* 2nd edn (Berlin: Springer)
[4] Hugdal H G and Berg P 2015 Numerical determination of the eigenenergies of the Schrodinger equation in one dimension *Eur. J. Phys.* **36** 045013
Chow P C 1972 Computer solutions to the Schrodinger equation *Am. J. Phys.* **40** 730
Bolemon J S 1972 Computer solutions to a realistic one-dimensional Schrödinger equation *Am. J. Phys.* **40** 1511
[5] Sra S, Nowozin S and Wright S J 2012 *Optimization for Machine Learning* (Cambridge, MA: MIT Press)
[6] Cooney P J, Kanter E P and Vager Z 1981 Convenient numerical technique for solving the onedimensional Schrodinger equation for bound states *Am. J. Phys.* **49** 76
Randles K, Schroeder D V and Thomas B R 2019 Quantum matrix diagonalization visualized *Am. J. Phys.* **87** 857
[7] Gulliksson M, Ögren M, Oleynik A and Zhang Y 2018 Damped dynamical systems for solving equations and optimization problems *Handbook of the Mathematics of the Arts and Sciences* ed B Sriraman (Berlin: Springer)
[8] Baravdish G, Svensson O, Gulliksson M and Zhang Y 2019 Damped second order flow applied to image denoising *IMA J. Appl. Math.* **84** 1082
[9] Sandin P, Ögren M and Gulliksson M 2016 Numerical solution of the stationary multicomponent nonlinear Schrodinger equation with a constraint on the angular momentum *Phys. Rev.* E **93** 033301

[10] Gulliksson M 2017 The discrete dynamical functional particle method for solving constrained optimization problems *Dolomites Res. Notes Approx.* **10** 6 (https://drna.padovauniversitypress.it/system/files/papers/Gulliksson_DRNA2017.pdf)
[11] Gulliksson M, Edvardsson S and Lind A 2013 The dynamical functional particle method (arXiv:1303.5317)
[12] Gelfand I M and Fomin S V 2000 *Calculus of Variations* (New York: Dover)
[13] Begout P, Bolte J and Jendoubi M 2015 On damped second-order gradient systems *J. Differ. Equ.* **259** 3115
[14] Hairer E, Lubich C and Wanner G 2006 *Geometric Numerical Integration* 2nd edn (Berlin: Springer)
[15] Poljak B T 1964 Some methods of speeding up the convergence of iterative methods *Akademija Nauk SSSR Z. Vycisl. Mat. Matematicoskoi Fiziki* **4** 791
[16] Sandro I, Valerio P and Francesco Z 1979 A new method for solving nonlinear simultaneous equations *SIAM J. Numer. Anal.* **16** 779
[17] Mclachlan R, Modin K, Verdier O and Wilkins M 2014 Geometric generalisations of SHAKE and RATTLE *Found. Comput. Math.* **14** 339
[18] Schiff L I 1968 *Quantum Mechanics* 3rd edn (New York: McGraw-Hill)
[19] Abramowitz M and Stegun I A (eds) 1964 *Handbook of Mathematical Functions* (National Bureau of Standards Publication) (http://people.math.sfu.ca/~cbm/aands/abramowitz_and_stegun.pdf)
[20] Pethick C J and Smith H 2008 *Bose–Einstein Condensation in Dilute Gases* 2nd edn (Cambridge: Cambridge University Press)
[21] Jackson A D, Smyrnakis J, Magiropoulos M and Kavoulakis G M 2011 Solitary waves and yrast states in Bose–Einstein condensed gases of atoms *Europhys. Lett.* **95** 30002